Collagen-CMC xerogels for methylene blue adsorption: kinetic and thermodynamic parameters

D.A. Cabrera-Munguia[1], E.R. Rocha-Vazquez[1], M.I. León-Campos[1], L.F. Cano-Salazar[1], T.E. Flores-Guia[1] & J.A. Claudio-Rizo[1*]

[1]Materiales Avanzados, Facultad de Ciencias Químicas, Universidad Autónoma de Coahuila, Saltillo, Coahuila, México.
Corresponding Author (J.A. Claudio-Rizo) Email: jclaudio@uadec.edu.mx[*]

ABSTRACT

Collagen-carboxymethylcellulose (CMC) xerogels were obtained by drying the corresponding hydrogels at an environmental temperature, which were synthesized through the microemulsion method. The mass percentage of carboxymethylcellulose to collagen was varied (X=0, 8.3, 16.6, and 33.3 % m). The physicochemical characterization demonstrated the crosslinking between collagen's amine groups with the hydroxyl group of the carboxymethylcellulose (ATR-FTIR), which is confirmed by the presence of fibrillar structures embedded on flat surfaces (SEM), whose amorphous crystalline structure is incremented with the CMC amount (WAXS). The methylene blue (MB) adsorption experiments data are better adjusted to Natarajan and Khalaf equation which is indicative of adsorption kinetics of first order. In addition, the adsorption data was adjusted to the Langmuir isotherm, the R_L parameter range from 0 to 1, which is indicative of a favorable adsorption. The Gibbs free energy was positive which is in line with an irreversible ($\Delta S>0$) and endothermic process ($\Delta H>0$). Interestingly, when the adsorption temperature is incremented (50º C) the R_L parameter ranges from 0 to 1, a characteristic of an irreversible adsorption, which implies a chemisorption of methylene blue on the xerogel surface favored by temperature instead of a physisorption process when a low temperature (30ºC) is applied.

Keywords: Carboxymethylcellulose; Collagen; Xerogels; Methylene Blue; Adsorption; Langmuir Isotherm; Chemisorption; Enthalpy; Entropy.

1. Introduction

Aniline blue, alcian blue, basic fuchsin, methylene blue, crystal violet, and congo red are some examples of synthetic dyes that are in high demand in the textile and clothing industries. Methylene blue (MB) is one of the most popular cationic dyes, which can also be applied for dyeing paper and leather, as well as in cosmetics, food, and pharmaceutical industries [1,2]. Methylene blue (MB) is an aromatic heterocyclic chemical compound with molecular formula $C_{16}H_{18}ClN_3S$ that is not usually eliminated in a standard water treatment process due to its high stability to temperature, light, oxidizing agents, and microbial attack [3].

Among the most relevant technologies for dying wastewater treatment, outstanding filtration, adsorption, chemical reduction, membrane filtration, coagulation/flocculation, ion-exchange removal, the oxidation technologies (photocatalysis, ozonation, UV-fenton, electrocoagulation), and biological sequential process (anaerobic-aerobic) [2,4]. However, the adsorption has been proved to be the most efficient and economical way to remove textile dyes with chemical structures based on aromatic compounds [4].

The adsorption is a mass transfer phenomenon in which the dye molecules are removed from the water through a solid phase, by physicochemical interactions between the adsorbed species (adsorbate) and the solid surface (adsorbent). To determine the maximum adsorption capacity of the adsorbent material, the adsorption experimental data is compared with the Langmuir and/or the Freundlich model isotherms to assess pollutant adsorption [5].

Some examples of materials applied as adsorbents are siliceous materials, clays, zeolites, chitin, chitosan, metal oxide-based nanomaterials (CuO, Fe_3O_4, ZnO), carbon-based nanomaterials and industrial and agricultural wastes [5,6]. Hydrogels and their xerogels (dried form) are reticulated polymers that can absorb a large amount of water due to their content of hydrophilic groups that can function as adsorptive sites for removing dyes [7]. The removal

mechanism for dye involves electrostatic, ion exchange, chemisorption, hydrogen bonding, hydrophobic, and complexation interactions between dyes and adsorbents [8].

Hydrogels based on natural polymers are typically applied in biomedical and pharmaceutical applications due to their high biocompatibility and biodegradability. But their high content of ionic and non-ionic functional groups like carboxylic acid, amine, hydroxyl, and sulfonic acid in their chemical structure makes them suitable for being excellent adsorbents [9]. In this way, the application of biopolymers such as collagen and carboxymethyl cellulose (CMC) with a high content of hydrophilic groups ($-NH_2$ and OH^-) to prepare xerogels (Figure 1) for their hydrogels synthesized by the microemulsion method [9-12]. It can be helpful as a biodegradable adsorbent for MB removal, aiming to reduce the generation of new polluting wastes.
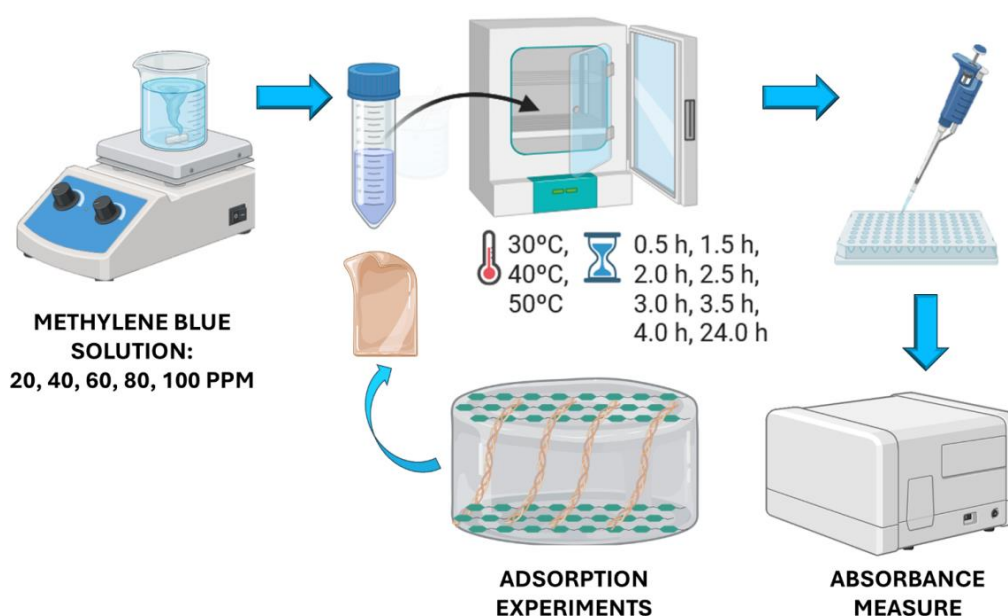

Figure 1. Collagen-CMC Xerogels for Methylene Blue Adsorption

1.1. Study Objectives

1) To synthesize collagen-CMC xerogels, varying the amount of CMC (X=0, 8.3, 16.6, and 33.3 % m).

2) To characterize xerogels by ATR-FTIR, WAXS and SEM to analyze the chemical crosslinking, crystalline and textural properties of xerogels.

3) To evaluate the adsorptive properties of collagen-CMC xerogels in MB adsorption, varying the colorant concentration.

4) To adjust the kinetic data of MB adsorption to a model and select the xerogel with the highest kinetic value.

5) To make a thermodynamic study for MB adsorption, changing the temperature and colorant concentration with the best xerogel formulation.

2. Materials and Methods

In this research, collagen type I was extracted by enzymatic hydrolysis with pepsin, as reported elsewhere [13], obtaining specific molecular weights of 110 kDa and 220 kDa. The crosslinking agent was based on polyurethane

with a molecular weight of 3000 to 7500 g mol^{-1}. This was synthesized from glycerol ethoxylate and 1,6-hexamethylene diisocyanate, using the procedure reported elsewhere [14]. All the reagents used for collagen extraction and the synthesis of the crosslinking agent, as well as methylene blue (MB, 319.85 g mol-1) and sodium carboxymethyl cellulose (CMC, 250 kDa), were bought from Merck. The reliable CTR Scientific supplied essential chemicals for preparing the PBS 10X solution, such as sodium chloride, potassium chloride, sodium hydroxide, monopotassium phosphate, and sodium acid phosphate.

2.1. Synthesis of Collagen-CMC Xerogels

The CMC solution was prepared by dissolving 0.5g of CMC in 100 mL of deionized water. The hydrogel was synthesized using the microemulsion method using a 24-well microplate as a mold [15]. Then, 1 mL of collagen and 100, 200, or 400 µL of CMC were added to each well (Table 1). Then, 20 µL of crosslinking agent and 250 µL of PBS 10X were added to each well. When the process is accomplished, the 24-well microplate is placed in an incubator at 37ºC for at least 4 h. The hydrogels obtained were dried at ambient temperature for future use.

Table 1. Chemical Composition of Collagen-CMC Xerogels

Formulation	Colágeno, mg	CMC, mg	CMC, µL	Masa CMC, %
CMC-0	6	0.0	0	0
CMC-100	6	0.5	100	8.3
CMC-200	6	1.0	200	16.7
CMC-400	6	2.0	400	33.3

2.2. Physicochemical Characterization of Xerogels

The functional groups involved in the entanglement of the collagen, CMC, and the crosslinking agent were studied in the xerogels by infrared radiation using a *Perkin Elmer Frontier* spectrophotometer with an attenuated total reflectance accessory (ATR); the spectra were acquired in a range from 4000 to 600 cm^{-1} with a resolution of 4 cm^{-1}. The crystalline properties of xerogels were analyzed by Wide Angle X-ray Scattering (WAXS) in a *Bruker D8 Advance* diffractometer with an SDD 160 detector and X-ray source Cu Kα (λ=1.5418 Å), the diffractograms were obtained in a range from 10 to 50º at 2θ with a step size of 0.02. The Scanning Electron Microscopy (SEM) study was done in a *JEOL* microscope JSM 6520V/LGS model with a voltage of 15 kV; the xerogel samples were covered with graphite to be observed.

2.3. Methylene Blue Adsorption Experiments

All MB adsorption experiments were done in triplicate. An MB of 100 ppm was used as a stock solution to make the calibration curve. The relation between absorbance and concentration in parts per million (ppm) follows the linear equation (Eq. 1):

$$A = 0.1985 + 0.0319 ppm \qquad \text{Eq. (1)}$$

A represents the absorbance measured at 680 nm in a *ThermoScientific MultiSkan Sky* spectrophotometer, and *ppm* represents the MB concentration in parts per million. In the first part of the experiments, the kinetic adsorption curve was obtained at 40ºC from each material using in a typical experiment a 20 mL solution with an initial

OPEN ACCESS

concentration of 100 ppm and 0.1 g of xerogel, and taking samples of 200 μL at 0.5 h, 1.5h, 2.0 h, 2.5 h, 3.0 h, 3.5 h, and 4.0 h to measure the absorbance. The experimental data was adjusted to different kinetic models to find the suitable model and compare each xerogel formulation's kinetic constant adsorption value [16].

Once the best formulation was selected, it was used to perform a thermodynamic study, varying the concentration (20, 40, 60, 80 and 100 ppm) and adsorption temperature (30, 40 and 50ºC), to adjust the experimental data to the Langmuir isotherm and found the adsorption capacity (q_m) and the Langmuir adsorption constant (K_L), this latter is applied to find the Gibbs free energy of the adsorption, and with the temperature variation, entropy and enthalpy for MB adsorption can be calculated [17].

3. Results and Discussion

3.1. ATR-FTIR

The ATR-FTIR spectra of collagen-CMC(X) xerogels are shown in Figure 2. All spectra generally show the stretching signals for the νNH and νOH vibration of the amino, alcohol, and carboxylic acid groups present in collagen and CMC between 3600–3000 cm^{-1}. The signals at around 2860 and 2930 cm^{-1} belong to the -CH vibration related to the hydrocarbon skeleton of collagen [18]. The band at around 1744 cm^{-1} is associated with the urea carbonyl bond formed during the crosslinking reaction between isocyanate groups of the crosslinking agent that react with the primary amine groups of collagen; this band is practically maintained when CMC is added to the collagenic matrix [15]. However, the intensity of the typical bands of polypeptides, at around 1635 cm-1 (Amide I), 1536 cm-1 (Amide II), and 1392 cm-1 (Amide III), is decreased when CMC is incorporated into the collagen matrix. This phenomenon is duplicated in the broadband between 3600–3000 cm^{-1}. This suggests that collagen and CMC are crosslinked by hydrogen bonding between collagen's amine groups and carboxyl and hydroxyl functional groups from CMC. Finally, the bands between 1400 to 1000 cm^{-1} are related to the -CH and -CH3 deformation vibration present in the collagen amino acids glycine, proline and hydroxyproline, mainly [19].
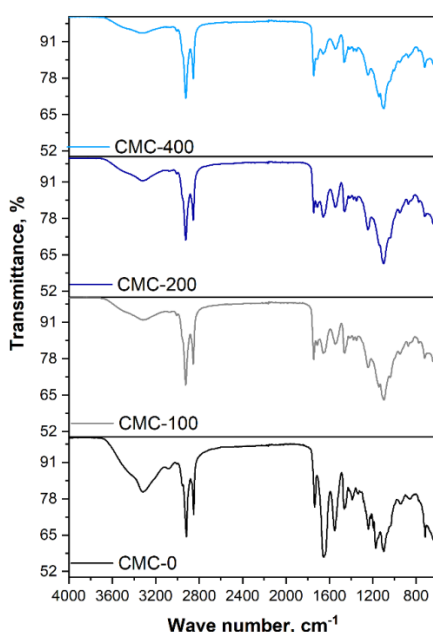

Figure 2. ATR-FTIR Spectra of Collagen-CMC Xerogels

3.2. XRD

The crystalline structure of xerogels was studied by WAXS (Figure 3). The diffraction patterns of collagen-CMC(X) xerogels indicate a broad band at 2θ between 20º and 30º, which is attributed to the CMC incorporation into the collagenic matrix, as is reported in other studies with other polysaccharides [20, 21]. There are also three additional diffraction peaks at 27.5º, 31.82º, and 45.5º at 2θ, related to collagen's crystalline and fibrillar structure when the crosslinking agent entangles it. However, the diffraction peak located at 45.5º is increased when the CMC is also increased, which suggests the hydrogen bonding between the hydrophilic groups of collagen and CMC; this is in line with the ATR-FTIR results.
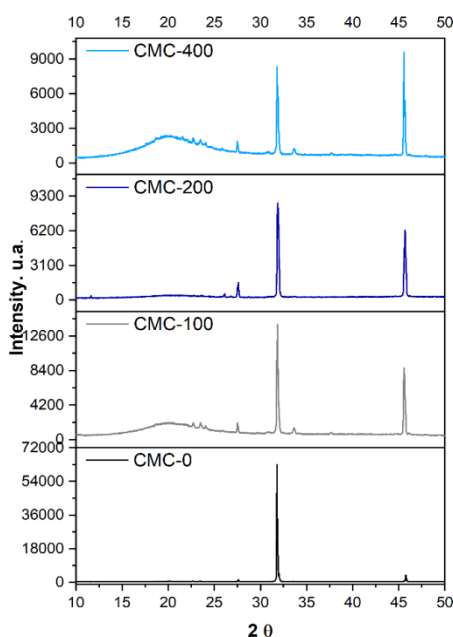

Figure 3. XRD of Collagen-CMC(X) Xerogels

3.3. SEM

The SEM micrographs (Figure 4) show fibrillar structures occluded in dispersed aggregates from collagen, with irregular relief and interconnected porosity is observed for the sample without CMC [21]. When the amount of CMC is increased, the reliefs lose their porosity except for CMC-100. Also, the fibrillar structures become short, and there are fewer collagen aggregates, becoming a more amorphous surface, which concurs with the WAXS results.

3.4. Adsorption Kinetic Parameters

The kinetic data of collagen-CMC(X) xerogels were obtained at 40ºC with an initial solution of MB of 100 ppm (mg L^{-1}). The kinetic curves are plotted in Figure 5; these experimental data were better adjusted to the Natarajan and Khalaf (Eq. 2) kinetic model [16]:

$$\log\left(\frac{c_0}{c_t}\right) = \left(\frac{k}{2.303}\right) \qquad \text{Eq. (2)}$$

C_0 and C_t are ppm (mg L^{-1}) concentrations at zero time and at any time, respectively. The adsorption kinetic constant of first order (k) in units of min^{-1}. The Table 2 shows the k value for each xerogel formulation and the linear

correlation factor (R^2). The kinetic constant value increases from 7 to 30% when the CMC-100 formulation is applied in adsorption compared to the other materials. This result is related to the better collagen aggregate dispersion and porosity preservation in CMC-100 xerogel.
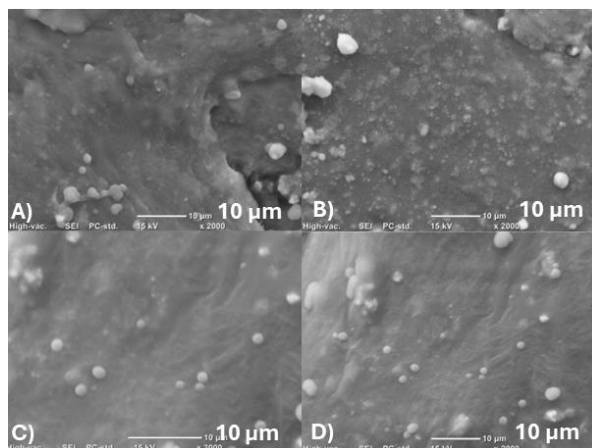

Figure 4. SEM Micrographs of Collagen-CMC(X) Xerogels: A) CMC-0, B) CMC-100, C) CMC-200 and D) CMC-400
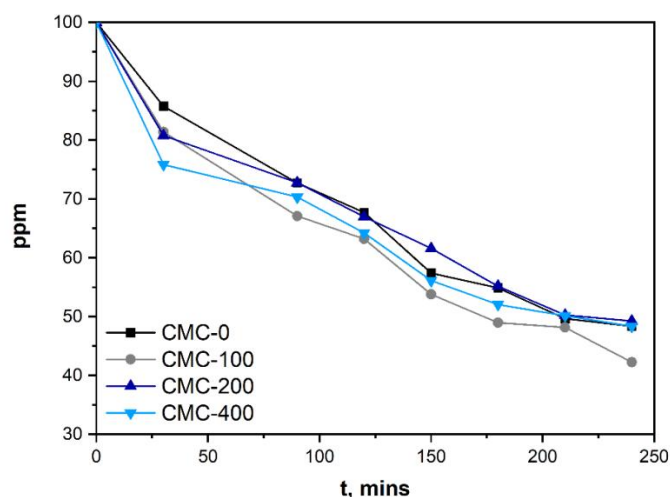

Figure 5. Methylene Blue Adsorption over Collagen-CMC(X) Xerogels at 40ºC

Table 2. Kinetics Adsorption Constant of Collagen-Cellulose Xerogels

Formulación	$k \times 10^3$, min^{-1}	R^2
CMC-0	1.2579	0.9794
CMC-100	1.3478	0.9828
CMC-200	1.1180	0.9814
CMC-400	1.0349	0.9616

3.5. Adsorption Thermodynamic Parameters

The Langmuir adsorption theory states that adsorption occurs at specific homogeneous sites inside the adsorbent, and once the adsorbate occupies the site, another adsorbate can't occupy the same site. The Langmuir model is helpful to predict the performance of different adsorbents. The mathematical expression of the Langmuir model (Eq. 3) [17]:

$$\frac{C_e}{q_e} = \frac{1}{q_m K_L} + \frac{C_e}{q_m} \qquad \text{Eq. (3)}$$

Where K_L is the Langmuir constant (L mg^{-1}) and its value indicates the affinity between the adsorbate and the adsorbent. The C_e (mg L^{-1}) parameter is the concentration of the adsorbate at the equilibrium, q_e (mg g^{-1}) is the adsorption capacity at the equilibria and q_m parameter is the maximum adsorption capacity (saturated monolayer) in mg g^{-1}. The equilibria parameter R_L (Eq. 4) is calculated as [17]:

$$R_L = \frac{1}{1 + K_L C_0} \qquad \text{Eq. (4)}$$

The value of $R_L > 1$ is indicative of an unfavorable isotherm, $R_L = 1$ expresses a linear isotherm, values of $0 < R_L < 1$ indicate a favorable isotherm, while a $R_L = 0$ is referred to as an irreversible isotherm (chemisorption).

Figure 6 shows the C_e plotted against the C_e/q_e ratio at 30, 40 and 50ºC, from the slope is obtained the q_m and K_L is obtained from the intercept. Table 3 shows the values of q_m and K_L, this latter is used for the calculus of the Gibbs free energy (ΔG), which is determined by Eq. 5:

$$\Delta G = -RT \ln K_L \qquad \text{Eq. (5)}$$

At the same time the relation between ΔG, enthalpy (ΔH) and entropy (ΔS) are given by Eq. 6:

$$\Delta G = \Delta H - T\Delta S \qquad \text{Eq. (6)}$$

The results presented in Table 3 indicate a very low maximum adsorption capacity compared to the 321 mg/g reported elsewhere [11]. This can be explained by $\Delta G > 0$, indicating that the adsorption is a nonspontaneous phenomenon associated with an irreversible ($\Delta S > 0$) and endothermic process ($\Delta H > 0$). When the temperature increases, the value of K_L is incremented to fifteen to nineteen times, resulting in an R_L value very close to zero. This suggests that the adsorption changes to physisorption to chemisorption when the temperature is increased.
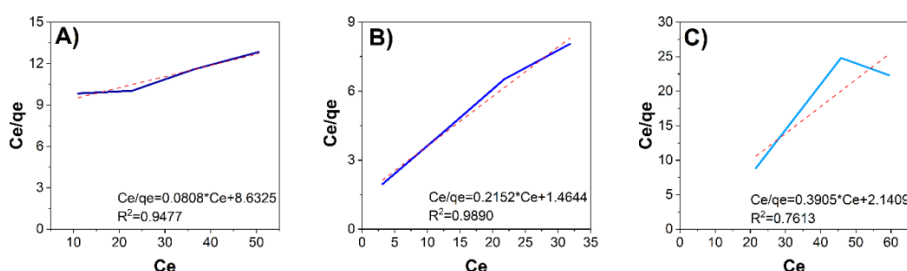

Figure 6. Langmuir Isotherm at A) T=30ºC, B) T=40ºC and C) T=50ºC

Table 3. Parameters of Langmuir Model

Temperature, K	q_m, mg/g	K_Lx10^3, L/mg	ΔG, kJ/mol	ΔH, kJ/mol	ΔS, J/mol
303	12.4	9.4	11.8		
313	4.6	146.9	5.0	121.9	366.7
323	2.6	182.4	4.6		

4. Conclusion

The increment in the mass percentage of CMC in the collagenic matrix caused an augmentation in the hydrogen bonding interactions between the CMC's carboxyl groups and collagen's amine groups, as the ATR-FTIR spectra

showed a diminution in the bands associated with hydroxyl, amine, and amide functional groups. The SEM micrographs indicated fibrillar structures embedded into plane surfaces with reliefs with low porosity, which is in line with the amorphous structures found in the WAXS analysis. Also, the MB adsorption data were adjusted to the Natarajan and Khalaf model corresponding to a first order, where the formulation CMC-100 showed the highest kinetic value associated with the preservation of collagen porosity in this material.

Then, CMC-100 was used to evaluate in a thermodynamic study, to adjust the experimental data with the Langmuir parameters, and a maximum adsorption capacity of 12.4 mg/g at 30ºC. Interestingly, when the adsorption temperature is increased, the equilibrium constant for adsorption (K_L) is also augmented resulting in a better interaction between adsorbate and adsorbent and thus a chemisorption process. This result is in correspondence with an endothermic($\Delta H>0$), irreversible($\Delta S>0$), and non-spontaneous ($\Delta G>0$) adsorption process.

5. Future Recommendations

1) The synthesis of other xerogel formulations with collagen as a matrix, with other polysaccharides that enhance the swelling, textural, and adsorptive properties of xerogels.

2) The synthesis of xerogel formulations based on polysaccharides with the addition of metal-organic frameworks (MOFs) that serve as a reticulation point to enhance their mechanical stability.

3) To evaluate the use of adsorbents commonly considered as residues, such as eggshells as low-cost alternatives.

4) To study the adsorption of other colorants of azo and indole nature, such as Congo red and Indigo Carmine, respectively.

References

[1] Oladoye, P.O., Ajiboye, T.O., Omotola, E.O., & Oyewola, O.J. (2022). Methylene blue dye: Toxicity and potential elimination technology from wastewater. RINENG, 16: 100678. https://doi.org/10.1016/j.rineng.2022. 100678.

[2] Din, M.I., Khalid, R., Najeeb, J., & Hussain, Z. (2021). Fundamentals and photocatalysis of methylene blue dye using various nanocatalytic assemblies- a critical review. J Clean Prod., 298: 126567. https://doi.org/10.1016/j.jcle pro.2021.126567.

[3] Khan, I., Saeed, K., Zekker, I., et al. (2022). Review on Methylene Blue: Its Properties, Uses, Toxicity and Photodegradation. Water (Switzerland), 14(2): 242. https://doi.org/10.3390/w14020242.

[4] Shabir, M., Yasin, M., Hussain, M., et al. (2022). A review on recent advances in the treatment of dye-polluted wastewater. J Ind Eng Chem., 112: 1–19. https://doi.org/https://doi.org/10.1016/j.jiec.2022.05.013.

[5] Rashid, R., Shafiq, I., Akhter, P., et al. (2021). A state-of-the-art review on wastewater treatment techniques: the effectiveness of adsorption method. Environ Sci Pollut Res., 28: 9050–9066. https://doi.org/10.1007/s11356-021-12395-x.

[6] Zhou, Y., Lu, J., Zhou, Y., & Liu, Y. (2019). Recent advances for dyes removal using novel adsorbents: A review. Environ Pollut., 252: 352–365. https://doi.org/10.1016/j.envpol.2019.05.072.

[7] Yang, Y., Zhu, Q., Peng, X., et al. (2022). Hydrogels for the removal of the methylene blue dye from wastewater: a review. Environ Chem Lett., 20: 2665–2685. https://doi.org/10.1007/s10311-022-01414-z.

[8] Hu, X.S., Liang, R., & Sun, G. (2018). Super-adsorbent hydrogel for removal of methylene blue dye from aqueous solution. J Mater Chem A Mater., 6: 17612–17624. https://doi.org/10.1039/c8ta04722g.

[9] Kurdtabar, M., Peyvand Kermani, Z., & Bagheri Marandi, G. (2015). Synthesis and characterization of collagen-based hydrogel nanocomposites for adsorption of Cd^{2+}, Pb^{2+}, methylene green and crystal violet. Iran Polym J (English Edition), 24: 791–803. https://doi.org/10.1007/s13726-015-0368-6.

[10] Ayouch, I., Kassem, I., Kassab, Z., et al. (2021). Crosslinked carboxymethyl cellulose-hydroxyethyl cellulose hydrogel films for adsorption of cadmium and methylene blue from aqueous solutions. Surf Interfac., 24: 101124. https://doi.org/10.1016/j.surfin.2021.101124.

[11] Hooshvar, M., Bagheri Marandi, G., & Taghvay Nakhjiri, M. (2024). Collagen-Based Hydrogel Nanocomposite as Adsorbent for Methylene Blue and Crystal Violet Removal from Aqueous Solution: Isotherm, Kinetic, and Thermodynamic Studies. Water Air Soil Pollut., 235: 161. https://doi.org/10.1007/s11270-024-06971-3.

[12] Zhao, H., Liang, Z.X., & Gao, Z.Z. (2022). Facile preparation of floatable carboxymethyl cellulose-based composite hydrogel for efficient removal of organic dyes. Colloid Interfac Sci Comm., 49: 100637. https://doi.org/10.1016/j.colcom.2022.100637.

[13] Claudio-Rizo, J.A., Rangel-Argote, M., Castellano, L.E., et al. (2017). Influence of residual composition on the structure and properties of extracellular matrix derived hydrogels. Mat Sci Eng C-Mater., 79: 793–801. https://doi.org/10.1016/j.msec.2017.05.118.

[14] Mendoza-Novelo, B., Mata-Mata, J.L., Vega-González, A., et al. (2014). Synthesis and characterization of protected oligourethanes as crosslinkers of collagen-based scaffolds. J Mater Chem B, 2: 2874–2882. https://doi.org/10.1039/c3tb21832e.

[15] Claudio-Rizo, J.A., Hernandez-Hernandez, N.G., Cano-Salazar, L.F., et al. (2021). Novel semi-interpenetrated networks based on collagen-polyurethane-polysaccharides in hydrogel state for biomedical applications. J Appl Polym Sci., 138(4): 49739. https://doi.org/10.1002/app.49739.

[16] Musah, M., Azeh, Y., Mathew, J., et al. (2022). Adsorption Kinetics and Isotherm Models: A Review. CaJoST, 4: 20–26. https://doi.org/10.4314/cajost.v4i1.3.

[17] Gao, J.J., Qin, Y.B., Zhou, T., et al. (2013). Adsorption of methylene blue onto activated carbon produced from tea (*Camellia sinensis* L.) seed shells: Kinetics, equilibrium, and thermodynamics studies. J Zhejiang Univ Sci B, 14: 650–658. https://doi.org/10.1631/jzus.B12a0225.

[18] Guzmán-Chávez, M.L., Claudio-Rizo, J.A., Caldera-Villalobos, M., et al. (2022). Novel bioactive collagen-polyurethane-pectin scaffolds for potential application in bone regenerative medicine. Appl Surf Sci Adv., 11: 100317. https://doi.org/10.1016/j.apsadv.2022.100317.

[19] Caldera-Villalobos, M., Claudio-Rizo, J.A., Rodríguez-Estrada, V.A., et al. (2023). Effect of the content of starch on the biocompatibility, bacterial inhibition, and drug release performance of semi-IPN collagen-polyurethane hydrogels. J Macromol Sci Part A: Pure Appl Chem., 60: 124–134. https://doi.org/10.1080/10601325.2023.2166842.

[20] Lopéz-Martínez, E.E., Claudio-Rizo, J.A., Caldera-Villalobos, M., et al. (2022). Hydrogels for Biomedicine Based on Semi-Interpenetrating Polymeric Networks of Collagen/Guar Gum: Synthesis and Physicochemical Characterization. Macromol Res., 30: 375–383. https://doi.org/10.1007/s13233-022-0047-3.

[21] Caldera-Villalobos, M., Ramos-Montañez, D.G., Cabrera-Munguía, D.A., et al. (2023). Biocompatible hydrogels comprised of collagen, chitosan and polyurethane with potential applications for wound healing and controlled drug release. Polym Int., 74(1): 9–19. https://doi.org/10.1002/pi.6590.